with a dihedral angle X corresponding to 48 ± 3° and 46 ± 2°, respectively.

A change of torsional angle occurs around a head-to-head bonding defect site, so that the structure resembles the planar zigzag conformation of PE around the defect site. Beyond it, the conformation reverts to TGTG′ or TXTX′. The helical winding direction can either remain the same or be reversed, in going through the defect site. If the defect is tail-to-tail, the TGTG′ or TXTX′ general pattern is retained everywhere along the chain. Some adjustment of the dihedral angles around the defect site takes place, to reduce the Y–Y repulsions.

The geometry of a VDY/VY chain segment with 10% VY is very similar to the geometry of the corresponding PVDY chain segment. A small percentage of VY comonomer should therefore not change the preferred chain conformation.

Acknowledgment. I thank A. F. Burmester, P. T. DeLassus, N. G. Rondan, and R. A. Wessling for many helpful discussions.

Registry No. PVDCl, 9002-85-1; PVDF, 24937-79-9; PVDBr, 51736-72-2; (VC)(VDCl) (copolymer), 9011-06-7; (VF)(VDF) (copolymer), 25101-40-0; (VB)(VBBr) (copolymer), 117828-31-6; CH_3F, 593-53-3; CH_2F_2, 75-10-5; CH_3Cl, 74-87-3; CH_2Cl_2, 75-09-2; $CHCl_3$, 67-66-3; CH_3Br, 74-83-9; CH_2Br_2, 74-95-3; $CHBr_3$, 75-25-2; CHF_3, 75-46-7.

References and Notes

(1) Clark, T. *A Handbook of Computational Chemistry*; Wiley: New York, 1985.
(2) Wessling, R. A. *Polyvinylidene Chloride*; Gordon and Breach Science Publishers: New York, 1977.
(3) Bicerano, J. *Macromolecules*, following paper in this issue.
(4) Flory, P. J. *Macromolecules* **1974**, *7*, 381–392.
(5) Coleman, M. M.; Wu, M. S.; Harrison, I. R.; Painter, P. C. *J. Macromol. Sci.-Phys.* **1978**, *B15*, 463–480.
(6) Wu, M. S.; Painter, P. C.; Coleman, M. M.; *Spectrochim. Acta* **1979**, *35A*, 823–833.
(7) Wu, M. S.; Painter, P. C.; Coleman, M. M. *J. Polym. Sci., Polym. Phys. Ed.* **1980**, *18*, 95–110.
(8) Wu, M. S.; Painter, P. C.; Coleman, M. M. *J. Polym. Sci., Polym. Phys. Ed.* **1980**, *18*, 111–120.
(9) Narita, S.; Okuda, K. *J. Polym. Sci.* **1959**, *38*, 270–272.
(10) Orchard, B. J.; Tripathy, S. K.; Pearlstein, R. A.; Hopfinger, A. J. *J. Comput. Chem.* **1987**, *8*, 28–38.
(11) Hutnik, M.; Suter, U. W. *Polym. Prepr. (Am. Chem. Soc., Div. Polym. Chem.)* **1987**, *28*, 293–294.
(12) Bicerano, J.; Clark, H. A. *Macromolecules* **1988**, *21*, 585–597.
(13) Bicerano, J.; Clark, H. A. *Macromolecules* **1988**, *21*, 597–603.
(14) Theodorou, D. N.; Suter, U. W. *Macromolecules* **1985**, *18*, 1467–1478.
(15) Theodorou, D. N.; Suter, U. W. *Macromolecules* **1986**, *19*, 139–154.
(16) Theodorou, D. N.; Suter, U. W. *Macromolecules* **1986**, *19*, 379–387.
(17) Elias, H.-G. *Macromolecules, Volume 1: Structure and Properties*, 2nd ed.; Plenum Press: New York, 1984.
(18) Suter, U. W.; Saiz, E.; Flory, P. J. *Macromolecules* **1983**, *16*, 1317–1328.
(19) Farmer, B. L.; Hopfinger, A. J.; Lando, J. B. *J. Appl. Phys.* **1972**, *43*, 4293–4303.
(20) Farmer, B. L.; Lando, J. B. *J. Macromol. Sci.-Phys.* **1975**, *B11*, 89–119.
(21) Tonelli, A. E. *Macromolecules* **1976**, *9*, 547–551.
(22) Tonelli, A. E. *Macromolecules* **1980**, *13*, 734–741.
(23) Tonelli, A. E. *Macromolecules* **1982**, *15*, 290–293.
(24) Tonelli, A. E.; Schilling, F. C.; Cais, R. E. *Macromolecules* **1981**, *14*, 560–564.
(25) Tonelli, A. E.; Schilling, F. C.; Cais, R. E. *Macromolecules* **1982**, *15*, 849–853.
(26) Ziman, J. M. *Principles of the Theory of Solids*, 2nd ed.; Cambridge University Press: Cambridge, 1972; Chapters 2 and 4.

Semiempirical Calculations Simulating Interacting Pairs of Chain Segments of Poly(vinylidene halide) and Vinylidene Halide/Vinyl Halide Copolymers

Jozef Bicerano

The Dow Chemical Company, Central Research, Materials Science and Development Laboratory, 1702 Building, Midland, Michigan 48674. *Received May 16, 1988*

ABSTRACT: As a continuation of previous work on isolated chain segments of PVDY and VDY/VY copolymers, the results of calculations on interacting pairs of chain segments are presented. Here, PVD denotes polyvinylidene and Y = F, Cl, or Br. The semiempirical AM1 technique was used first, to determine the heats of formation of individual chain segments and the charges on atoms occupying different types of valence environments. The stability of the isolated chain segments was found to decrease in the order Y = F ≫ Cl > Br. The model molecules with Y = Br had positive heats of formation. Replacement of one Y atom by H resulted in a slight decrease in stability for Y = F and a slight increase in stability for Y = Cl or Br. The intermolecular energies of pairs of rigid molecules were then minimized, by optimizing the distance between them and their relative orientations. A force field Hamiltonian with Lennard-Jones (6–12 potential) and electrostatic (Coulombic) energy terms was used for this purpose. The pairs of molecules were found to be antiparallel and perfectly aligned for Y = F and antiparallel but at a slight oblique angle for Y = Cl or Br. The intermolecular energy was attractive and comparable (−26 to −28 kcal/mol) for all three $C_{20}H_{22}Y_{20}$–$C_{20}H_{22}Y_{20}$ pairs. The intermolecular energy of $C_{20}H_{22}Y_{20}$–$C_{20}H_{23}Y_{19}$ was slightly lower (more attractive) for Y = F and considerably higher (less attractive) for Y = Cl or Br, compared to the corresponding $C_{20}H_{22}Y_{20}$–$C_{20}H_{22}Y_{20}$ pair. The Lennard-Jones energy was always at least 97% of the total intermolecular energy. The Coulombic energy can be expected to increase significantly in larger ordered assemblies of chains.

Introduction

The results of force field calculations on isolated chain segments of PVDY and of VDY/VY copolymers[1] were reported in the preceding paper.[2] The results of semiempirical quantum mechanical calculations on isolated chain segments, and valence force field calculations[3] on interacting pairs of chain segments, are presented in this manuscript. Here, PVD denotes polyvinylidene and Y is a halogen atom. PVDC denotes Y = Cl, and PVDB denotes Y = Br.

Simple force field calculations neglect subtle effects, such as hydrogen bonding and other types of polar interactions.

0024-9297/89/2222-1413$01.50/0

Table I
AM1 Results for $C_{12}H_{14}Y_{12}$ and $C_{12}H_{15}Y_{11}$ [a]

	$C_{12}H_{14}Y_{12}$			$C_{12}H_{15}Y_{11}$		
property	Y = F	Y = Cl	Y = Br	Y = F	Y = Cl	Y = Br
ΔH_f	-627.6	-102.4	58.8	-583.2	-105.7	42.4
EE	-42523.2	-38873.7	-37684.5	-39391.4	-35869.5	-34720.6
CCR	34968.8	32657.9	31715.5	32308.4	30013.4	29090.7
IP	11.7	11.2	10.0	11.7	10.9	9.9
q_H	0.123	0.132	0.131	0.125	0.126	0.125
$q_Y(CY_2)$	-0.158	-0.071	0.021	-0.162	-0.072	0.015
$q_Y(CHY)$				-0.145	-0.085	-0.001
$q_C(H_2)$	-0.265	-0.188	-0.168	-0.254	-0.183	-0.162
$q_C(H_3)$	-0.262	-0.230	-0.225	-0.261	-0.230	-0.225
$q_C(Y_2)$	0.288	0.044	-0.151	0.281	0.042	-0.153
$q_C(HY_2)$	0.226	-0.050	-0.261	0.227	-0.049	-0.261
$q_C(HY)$				0.080	-0.055	-0.159
μ	8.173	5.116	4.436	6.237	4.604	4.406

[a] ΔH_f is the final heat of formation in kcal/mol. EE is the electronic energy in eV. CCR is the core–core repulsion energy in eV. IP is the ionization potential in eV. q_H is the average Mulliken charge of all H atoms in a model molecule. $q_C(H_2)$ is the average Mulliken charge of all nonterminal C atoms bonded to two H atoms. The other Mulliken charges are also defined as averages over all atoms in the same type of bonding environment. μ denotes the dipole moment in D (debyes).

For example, studies of polymer–solvent interactions[1] suggest that the Lewis acidity of the PVDC chain dominates the interactions. In isolated chain segments of PVDY or VDY/VY copolymers, however, the presence of the bulky Y atoms causes steric repulsions to become the most important factors in determining the molecular geometry. Simple force field calculations were, therefore, able to give reasonable geometries and relative energies for isolated chain segments of PVDY and of VDY/VY copolymers.[2]

Polarization effects are very important in studying interchain interactions. More sophisticated computational techniques, consisting of a combination of semiempirical quantum mechanical calculations and force field calculations utilizing more complex Hamiltonians, therefore had to be used.

Calculations and Results

Semiempirical Quantum Mechanical Calculations on Isolated Chain Segments. The AM1 (Austin Model 1) Hamiltonian available in version 3.10 of the MOPAC (Molecular Orbital Package) semiempirical quantum mechanical program was used. The model molecules which were previously utilized,[2] and which are also used in studying the interchain interactions, namely, $C_{20}H_{22}Y_{20}$ and $C_{20}H_{23}Y_{19}$, were too large to complete the AM1 calculations in a reasonable amount of time. The geometries of the smaller model molecules $C_{12}H_{14}Y_{12}$ and $C_{12}H_{15}Y_{11}$ were therefore optimized instead, starting from truncated versions of the geometries that were fully optimized by MM2 for $C_{20}H_{22}Y_{20}$ and $C_{20}H_{23}Y_{19}$.

Average Mulliken partial atomic charges were determined for each type of distinct bonding environment. These charges are needed as parameters in the force field treatment of the electrostatic portion of the interchain interactions. The most important results of these AM1 calculations are summarized in Table I.

Intermolecular Energetics. Geometries calculated previously[2] were used for the individual $C_{20}H_{22}Y_{20}$ and $C_{20}H_{23}Y_{19}$ model molecules. These molecules were assumed to be rigid bodies in the present work. The total intermolecular energy (E) of pairs of such rigid bodies was calculated as a function of their relative positions. E was taken to be the sum of Lennard-Jones (6–12 potential) energy (E_{LJ}) and electrostatic energy (E_e) terms: $E = E_{LJ} + E_e$.

$E_{LJ} = \sum_j\sum_i(-a_{ij}/r_{ij}^6 + b_{ij}/r_{ij}^{12})$ is a standard Lennard-Jones 6–12 potential energy. The summations ($\sum$) are over all distinct pairs of nonbonded atoms. The distance between atoms i and j is denoted by r_{ij}. The constant a_{ij} characterizes the attractive interaction, caused by mutual polarization effects, between atoms i and j, even when these two atoms are neutral. The constant b_{ij} characterizes the very steep hard-sphere steric repulsion that prevents nonbonded pairs of atoms from coming too close to one another. These constants are determined semiempirically. Several sets of a_{ij} and b_{ij} are available in CHEMLAB-II. Only set Z (Hopfinger's hard potential) had all the needed parameters for each of the six systems of interest and was therefore used in the calculations.

$E_e = (-c/\epsilon)\sum_j\sum_i[(q_iq_j)/r_{ij}]$ is a standard Coulombic electrostatic potential. Here, c is a units conversion constant, ϵ is the dielectric constant assumed for the system, and q_i and q_j are the partial atomic charges. This energy term takes into account the fact that the atoms in a molecule might have nonzero net charges, resulting in electrostatic interactions between them, in addition to the polarization effects included in the Lennard-Jones energy.

The partial atomic charges obtained by the AM1 calculations were used for q_i. A small constant correction term was added to each charge to make each model molecule neutral. This correction term was needed because the model molecules used in AM1 calculations ($C_{12}H_{14}Y_{12}$ and $C_{12}H_{15}Y_{11}$) had different proportions of atoms in various types of bonding environments than the model molecules used in CHEMLAB-II calculations ($C_{20}H_{22}Y_{20}$ and $C_{20}H_{23}Y_{19}$). The ϵ value of 3.5 recommended in the program documentation was found to be adequate.

As discussed below, the electrostatic energy turned out to be much smaller than the Lennard-Jones energy for all six systems of interest. The use of a smaller but still reasonable value of ϵ (such as 1.5), or the use of substantially different atomic charges calculated by some other technique, would therefore not have changed the results significantly.

Another useful energetic quantity is δE, defined simply as the change in E resulting from the replacement of $C_{20}H_{22}Y_{20}$ by $C_{20}H_{23}Y_{19}$ as the second molecule in a pair. δE can be used as a semiquantitative indicator of the energetic effects of replacing some of the VDY by VY during polymerization.

Finally, it is useful to define the purely geometrical variable σ, which is a dissimilarity index equal to the root mean square deviation in a match of the structures of corresponding $C_{20}H_{22}Y_{20}$ and $C_{20}H_{23}Y_{19}$ molecules. A higher σ indicates a less exact match between the two

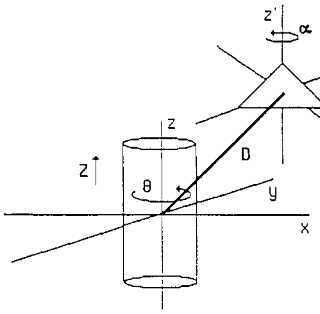

Figure 1. Geometrical parameters used in the optimization of intermolecular geometry. Reprinted from the CHEMLAB-II program manual, with the permission of Chemlab, Inc. (author of the manual) and Molecular Design Limited (distributor of CHEMLAB-II and the manual).

Table II
Results of Calculations of Intermolecular Energetics of $C_{20}H_{22}Y_{20}$ and $C_{20}H_{23}Y_{19}$[a]

fixed	mobile	E_{LJ}	E_e	E	δE	σ
$C_{20}H_{22}F_{20}$	$C_{20}H_{22}F_{20}$	−25.35	−0.51	−25.86		
$C_{20}H_{22}F_{20}$	$C_{20}H_{23}F_{19}$	−25.73	−0.82	−26.55	−0.69	0.08
$C_{20}H_{22}Cl_{20}$	$C_{20}H_{22}Cl_{20}$	−26.01	−0.24	−26.25		
$C_{20}H_{22}Cl_{20}$	$C_{20}H_{23}Cl_{19}$	−22.09	−0.40	−22.49	3.76	0.56
$C_{20}H_{22}Br_{20}$	$C_{20}H_{22}Br_{20}$	−28.08	−0.07	−28.15		
$C_{20}H_{22}Br_{20}$	$C_{20}H_{23}Br_{19}$	−23.84	−0.10	−23.94	4.21	0.63

[a] E_{LJ} is the Lennard-Jones (6–12 potential) energy. E_e is the electrostatic energy. E is the total energy. δE is the change in E resulting from the replacement of $C_{20}H_{22}Y_{20}$ by $C_{20}H_{23}Y_{19}$ as the mobile molecule. All energies are in kcal/mole. σ equals the root mean square deviation in a match of the structures of corresponding $C_{20}H_{22}Y_{20}$ and $C_{20}H_{23}Y_{19}$ molecules.

structures. σ is helpful in making correlations of the intermolecular energetics.

Geometry Optimization for Interacting Pairs of Chain Segments. Geometry optimization was performed by minimizing E as a function of intermolecular geometry. The PHBIMIN program in CHEMLAB-II was utilized. Six parameters are used by PHBIMIN to define the location of a "mobile molecule" relative to a "fixed molecule". These parameters are depicted in Figure 1. D is the distance between the reference points on the two chains. The centers of mass were taken to be the reference points in the present calculations. Z is the amount of translation of the mobile chain along its length dimension. The angle θ determines the particular orientation of the fixed molecule "seen" by the mobile molecule. The angle α determines the particular orientation of the mobile molecule "seen" by the fixed molecule. The angles β and γ, which are defined around two mutually perpendicular axes, both of which are also perpendicular to the axis of the mobile molecule, determine whether the two chains will be aligned (zero or small values) or at an oblique angle.

These six geometrical parameters were fully optimized. The calculations were repeated many times for each pair of model molecules, starting from various initial distances and orientations. This procedure greatly increases the probability but does *not* guarantee that the configuration found to have the lowest minimum E will either by the global minimum or be quite close to it. The results of these calculations are summarized in Table II.

Discussion

Isolated Chain Segments. A negative heat of formation indicates that a model molecule is stable relative to the elements constituting it, with these elements in their standard states. A positive heat of formation indicates that it is unstable relative to these elements. Once a molecule has been synthesized, however, kinetic barriers might also inhibit its dissociation. It might then be quite stable and not dissociate into its constituting elements, in spite of having a positive heat of formation.

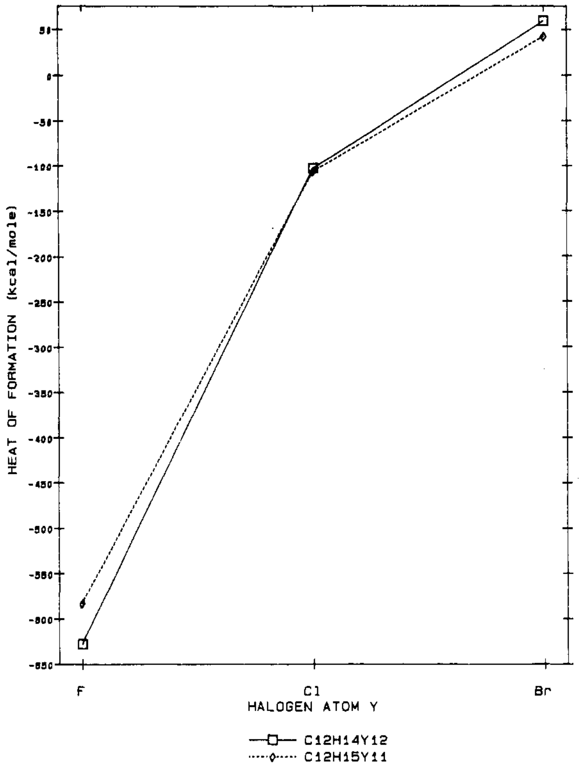

Figure 2. AM1 heat of formation as a function of the halogen atom.

As can be seen from Table I and Figure 2, the stability of the isolated chain segments decreases in the order Y = F ≫ Cl > Br. (Note that the sizes of the halogen atoms follow the reverse order (Br > Cl ≫ F).[4]) The heat of formation is negative for Y = F or Cl and positive for Y = Br. These trends are the result of the decrease in electronic stabilization (i.e., the less negative electronic energy (EE)) in the order Y = F ≫ Cl > Br. Core–core repulsion (CCR) energies decrease in the same order. The ionization potentials and dipole moments also follow the order Y = F > Cl > Br.

Replacement of one Y atom by an H atom results in an increase in the negative EE (i.e., a loss of electronic binding energy) and a decrease in the positive CCR (i.e., less core–core repulsion). The net effect is a slight decrease in stability for Y = F and a slight increase in stability for Y = Cl or Br. The effect on the ionization potentials is negligible. There is a marked reduction in the dipole moment for Y = F, a considerable reduction for Y = Cl, and a negligible reduction for Y = Br.

The charges on the H atoms are all positive and very similar. The average charges on the halogen atoms generally follow the order Br ≥ 0.0 > Cl ≫ F. Carbon atoms bonded to H always have a large negative charge, which is less negative in the order Y = F < Cl < Br. The charges on C atoms bonded to a Y atom are always large and positive for Y = F, always large and negative for Y = Br, and have small intermediate values for Y = Cl. The electronegativities of the elements[5] are 3.98 for F, 3.16 for Cl, 2.96 for Br, 2.55 for C, and 2.20 for H. The trends observed in the AM1 calculations are therefore in general agreement with the order (F > Cl > Br > C > H) of these electronegativities. The only exceptions are the carbon atoms bonded to Br, whose charges might have been expected, from simple electronegativity arguments, to be more positive, or less negative, than the charges on Br.

Significance of Calculations on Interacting Pairs of Chain Segments. Before discussing the conformations and energetics calculated for interacting pairs of chain segments, the limitations of such calculations will be summarized, to help place the results in proper perspective and to avoid drawing any unwarranted conclusions.

Even when the type of intermolecular geometry optimization utilized in this work is performed many times with the utmost diligence, the intermolecular geometries calculated can only be claimed to probably be close to the true minima, but they are not guaranteed to be so.

In addition, intermolecular calculations can be heavily dependent upon the selected intrachain conformations, unless intrachain geometries are optimized simultaneously with the interchain geometry. In the present case, the use of rigid intramolecular geometries, which is often a rather crude approximation, was deemed to be adequate at a semiquantitative level because, as discussed in the preceding paper,[2] the TGTG′ conformation calculated for the isolated chain segment of PVDF and the TXTX′ conformations calculated for PVDC and PVDB were all in very good agreement with experimental (crystallographic) results, which of course include all the intrachain *and* interchain effects.

Finally, because of differences in the physics of the systems, even if the objections described above are overcome, there can be significant differences between results calculated for only a pair of chain segments and results computed for larger ensembles more representative of the true intermolecular environment in the solid. For example, the Lennard-Jones energy is at least 97% of the total intermolecular energy for every chain pair system studied in this paper, so that all the major trends would have been the same if the electrostatic energy had been neglected altogether. On the other hand, the electrostatic (Coulombic) energy plays a significant role in the crystal, as demonstrated by the crystal-type calculations of Farmer et al.[6] on PVDF, which contains the most electronegative halogen atom and has the complications of polymorphism. (See the preceding paper[2] for a more detailed discussion of the factors determining the magnitude of electrostatic effects. These effects are also discussed in a later paragraph of this subsection.)

Such differences between the physics of chain pairs and many-chain assemblies clearly show that it is difficult, if not impossible, to get truly reliable chain-packing information from calculations based on only a pair of chains.

It is clear, therefore, that such relatively simple calculations on pairs of chain segments are useful mainly as bridges between the single-chain and the many-chain assembly levels of calculation. They provide information on the preferred modes of interaction of two chain segments in the absence of other chain segments. Comparison of their results with the results of isolated chain and multichain assembly calculations can facilitate the identification of which effects are primarily caused by (i) intrachain factors, (ii) the intrinsically preferred patterns of interaction between pairs of chains, and (iii) constraints and/or superpositions of effects induced by large-scale packing. The need to identify all these factors as clearly as possible has been shown in studies of the hierarchies of order and disorder in solids.[7] Such many-chain assembly calculations can be carried out by several methods. Examples of calculations on related systems include the work of Farmer et al. on PVDF[6] and the alternating copolymer of ethylene and tetrafluoroethylene,[8] and of Yemni and McCullough[9] on the energetics of orthorhombic-to-monoclinic phase transformations in polyethylene (PE). It should also be noted that CHEMLAB-II itself contains a routine (CHAINPACK) for packing polymer chains.

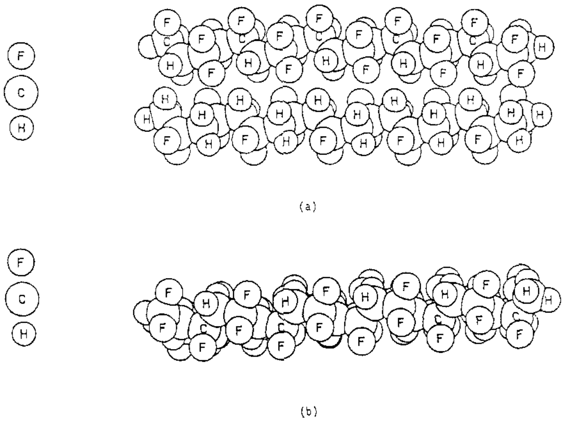

Figure 3. Space-filling illustrations of the $C_{20}H_{22}F_{20}$–$C_{20}H_{22}F_{20}$ pair: (a) a perspective showing both molecules; (b) an alternative perspective with one of the molecules behind the other and almost completely eclipsed by the molecule in the front. The closest *intermolecular* H–F distances range from 2.3 Å (at the chain ends) to 2.7 Å (at the centers of the chains).

A promising new technique for the prediction of polymer crystal structures and properties, using molecular mechanics and minimizing intermolecular and intramolecular energies simultaneously, has recently been introduced by Boyd's research group.[10] This method has been applied to predict structures and properties in reasonable agreement with experimental results for PE and poly(oxymethylene) (POM).[11] In this work,[11] a mutual induction model[12] was used to calculate the electrostatic (dipolar interaction) energy. There was no electrostatic energy contribution in PE, because the C–H bond was assumed to be nonpolar.[11] The electrostatic energy was the energy component with the largest magnitude in POM but only differed by an extremely small amount (0.3 kJ/mol of CH_2O units) between the hexagonal and orthorhombic polymorphs.[11]

Finally, an entirely different approach has been utilized by Blaisdell et al.[13] in a program (POLY-CRYST) which makes use of the translational and/or rotational symmetry in a polymer to compute ab initio molecular orbitals and utilize them in calculating several properties.

Conformations of Interacting Pairs of Chain Segments. As shown for the $C_{20}H_{22}F_{20}$–$C_{20}H_{22}F_{20}$ pair in Figure 3, the molecules are antiparallel and almost perfectly aligned for Y = F. Figure 3b shows that the intermolecular conformation can be viewed from a perspective in which one molecule is behind the other and almost completely eclipsed by it. The intermolecular conformation of the $C_{20}H_{22}F_{20}$–$C_{20}H_{23}F_{19}$ pair is almost identical with that of the $C_{20}H_{22}F_{20}$–$C_{20}H_{22}F_{20}$ pair and is therefore not shown.

The molecules are antiparallel but at a slight oblique angle for Y = Cl or Br, as depicted for the $C_{20}H_{22}Cl_{20}$–$C_{20}H_{22}Cl_{20}$ pair in Figure 4. Figure 4b shows that, in the perspective in which one molecule is behind the other, the molecule in the back is *not* almost completely eclipsed by the one in the front, and a considerable portion of it can still be seen. The size disparity between Cl and H, which is much greater than the size disparity between F and H, therefore appears to be sufficiently large to disfavor the parallel alignment. The intermolecular conformations of the $C_{20}H_{22}Cl_{20}$–$C_{20}H_{23}Cl_{19}$, $C_{20}H_{22}Br_{20}$–$C_{20}H_{22}Br_{20}$, and $C_{20}H_{22}Br_{20}$–$C_{20}H_{23}Br_{19}$ pairs are almost identical with that of the $C_{20}H_{22}Cl_{20}$–$C_{20}H_{22}Cl_{20}$ pair and therefore not shown.

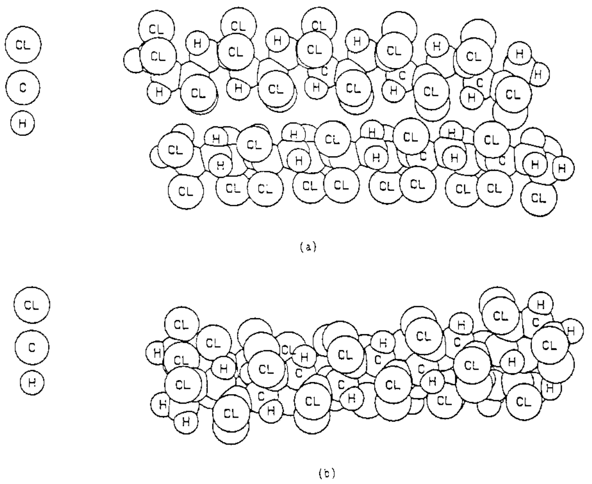

Figure 4. Space-filling illustrations of the $C_{20}H_{22}Cl_{20}$–$C_{20}H_{22}Cl_{20}$ pair: (a) a perspective showing both molecules; (b) an alternative perspective with one of the molecules behind the other but only partially eclipsed by the molecule in the front because the two molecules are at an oblique angle. As a consequence of the oblique angle, the closest *intermolecular* H–Cl distances vary much more than the closest H–F distances in Figure 3. The shortest close intermolecular H–Cl distance is 2.7 Å.

It is *not* obvious, from simple qualitative considerations, that utilization of much longer model molecules would necessarily result in significantly greater parallelization for Y = Cl or Br. The presence of more than two chains might force some additional parallelization; however, the energetic cost of forcing pairs of chains into the less favorable fully aligned pair geometries could be quite high.

A greater propensity of the chains to parallelize when Y = F than when Y = Cl may favor a higher percent crystallinity in PVDF. On the other hand, the incorporation of a much larger number of head-to-head bonding defect sites in chains of PVDF[14] may disfavor higher crystallinity in PVDF. Consequently, the crystallinities of PVDF and PVDC are comparable, with PVDC in general being slightly more crystalline than PVDF when prepared in the same manner.[15]

The size disparity between Br and H is only slightly larger than the size disparity between Cl and H. Consequently, the crystal structures of PVDC and PVDB can be expected to be much more similar than the crystal structures of PVDC and PVDF. This expectation is in agreement with the crystallographic data obtained by Narita and Okuda[16] by using highly oriented fibers.

The replacement of a halogen atom by an H atom in a nonterminal site did not result in any significant changes in the intermolecular conformations. The addition of a small percentage of VY comonomer (equivalent to 10% in these calculations) should therefore probably not cause any major changes in the packing patterns of these chains.

The arguments presented in this subsection were based solely on calculations on pairs of chain segments. They should, however, remain valid for larger assemblies of chain segments, and they describe the preferred *local* picture of intermolecular interactions on which large scale chain-packing effects will be superimposed, either reinforcing the trends that could be expected on the basis of calculations on pairs of chain segments or counteracting and modifying them. In other words, although predictions of chain packing based only on a pair of chain segments may often be incorrect, there is valuable information to be gained by determining to what extent they are applicable for a given system and why and how they fail when they do.

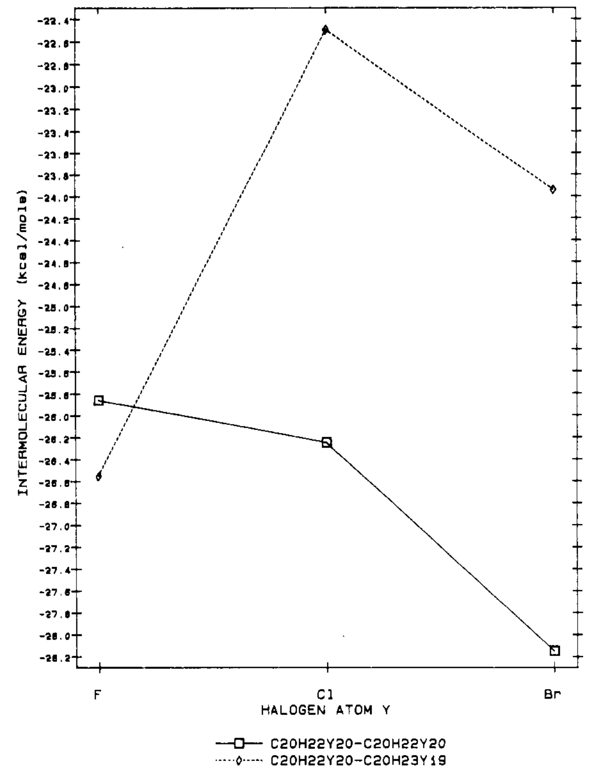

Figure 5. Intermolecular energy as a function of the halogen atom.

Energetics of Interacting Pairs of Chain Segments. As can be seen from Figure 5, the intermolecular energy (E) was attractive (−26 to −28 kcal/mol) for all three $C_{20}H_{22}Y_{20}$–$C_{20}H_{22}Y_{20}$ pairs. Since there are 20 monomer units in *two* $C_{20}H_{22}Y_{20}$ molecules, this E is equivalent to a stabilization energy of 1.3–1.4 kcal/mol per monomer unit.

In order to describe polymer stability quantitatively, it is necessary to perform more detailed calculations, including a calculation of the difference in the heat of formation between the monomer and the reactant. However, the enormous differences between the heats of formation of isolated chain segments of PVDF, PVDC, and PVDB, as calculated by AM1, along with the much smaller intermolecular pair energy, which is negative and comparable for each system, makes it possible to draw at least one important semiquantitative conclusion: the instability of PVDB is *not* caused by weak intermolecular binding but by the instability of its individual chains. This instability is manifested by the positive heat of formation, discussed above, of individual model molecules representing its isolated chain segments. In fact, the *inter*molecular stabilization slightly increases; i.e., E becomes slightly more negative, in the order Y = F < Cl < Br.

The E of $C_{20}H_{22}Y_{20}$–$C_{20}H_{23}Y_{19}$ pairs was slightly *more* negative for Y = F and considerably *less* negative for Y = Cl or Br than for the corresponding $C_{20}H_{22}Y_{20}$–$C_{20}H_{22}Y_{20}$ pair. As can be seen from Figure 6, the magnitude of δE is almost proportional to σ, which is an exact and quantitative index of the amount of mismatch between the geometries of corresponding $C_{20}H_{22}Y_{20}$ and $C_{20}H_{23}Y_{19}$ molecules. The significant loss of stabilization energy caused by the replacement of one Cl atom by an H atom shows that, although the intermolecular packing patterns might not change by the addition of a small percentage of comonomer, the intermolecular stabilization energy (and hence also the cohesive energy of the polymer) may decrease significantly.

Summary

The results of semiempirical quantum mechanical and

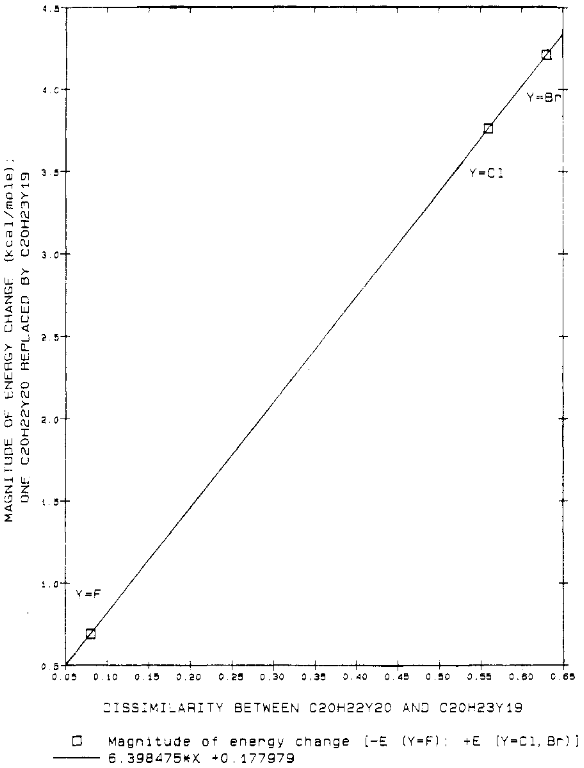

Figure 6. Energy change (δE) and index of dissimilarity (σ) as functions of the halogen atom.

valence force field calculations on interacting chain segments of PVDY and of VDY/VY copolymers were presented. Here, PVD denotes polyvinylidene and Y = F, Cl, or Br.

Simple force field calculations neglect subtle effects, such as hydrogen bonding and other types of polar interactions. Polarization effects are quite important in studying interchain interactions. More sophisticated computational techniques, consisting of a combination of semi-empirical quantum mechanical calculations and force field calculations utilizing more complex Hamiltonians, therefore had to be used.

The semiempirical AM1 technique was used first, to determine the heats of formation of individual chain segments and the charges on atoms occupying different types of valence environments. The stability of isolated chain segments was found to decrease in the order Y = F $\gg$ Cl $>$ Br. The model molecules with Y = Br had positive heats of formation. Replacement of one Y atom by H resulted in a slight decrease in stability for Y = F and a slight increase in stability for Y = Cl or Br.

Total intermolecular energies between rigid pairs of molecules were then minimized, by optimizing the distance between the two molecules in each pair and their relative orientations. A force field Hamiltonian with Lennard-Jones (6–12 potential) and electrostatic (Coulombic) energy terms was used for this purpose. The atomic charges estimated by AM1 were used as parameters in the electrostatic potential of this force field Hamiltonian.

The pairs of molecules were found to be antiparallel and perfectly aligned for Y = F and antiparallel but at a slight oblique angle for Y = Cl or Br. The intermolecular energy was attractive and comparable (−26 to −28 kcal/mol) for all three of the $C_{20}H_{22}Y_{20}$–$C_{20}H_{22}Y_{20}$ pairs. The intermolecular energy of $C_{20}H_{22}Y_{20}$–$C_{20}H_{23}Y_{19}$ was slightly lower (more attractive) for Y = F and considerably higher (less attractive) for Y = Cl or Br, compared to the corresponding $C_{20}H_{22}Y_{20}$–$C_{20}H_{22}Y_{20}$ pair. The Lennard-Jones energy was always at least 97% of the total intermolecular energy. The Coulombic energy can be expected to increase significantly in larger ordered assemblies of chains.

The results summarized above were used to draw as many conclusions as possible, by a static study of the intermolecular interactions of pairs of model molecules, about the chain-packing patterns and stabilities of PVDY and VDY/VY copolymers with a low percentage of comonomer. The limitations of such calculations, and the extent to which they might be useful when performed and interpreted very cautiously, were also discussed in detail.

Acknowledgment. I thank A. F. Burmester, H. A. Clark, P. T. DeLassus, I. R. Harrison, N. G. Rondan, and R. A. Wessling for many helpful discussions.

Registry No. PVDF, 24937-79-9; PVDC, 9002-85-1; PVDB, 51736-72-2; (VDF)(VF) (copolymer), 25101-40-0; (VDC)(VC) (copolymer), 9011-06-7; (VDB)(VB) (copolymer), 117828-31-6.

References and Notes

(1) Wessling, R. A. *Polyvinylidene Chloride*, Gordon and Breach Science Publishers: New York, 1977.

(2) Bicerano, J. *Macromolecules*, preceding paper in this issue.

(3) Clark, T. *A Handbook of Computational Chemistry*; Wiley: New York, 1985.

(4) Pauling, L. *The Nature of the Chemical Bond*, 3rd ed.; Cornell University Press: Ithaca, NY, 1973.

(5) Allred, A. L. *J. Inorg. Nucl. Chem.* **1961**, *17*, 215–221.

(6) Farmer, B. L.; Hopfinger, A. J.; Lando, J. B. *J. Appl. Phys.* **1972**, *43*, 4293–4303.

(7) Bicerano, J.; Adler, D. *Pure Appl. Chem.* **1987**, *59*, 101–144.

(8) Farmer, B. L.; Lando, J. B. *J. Macromol. Sci.-Phys.* **1975**, *B11*, 89–119.

(9) Yemni, T.; McCullough, R. L. *J. Polym. Sci., Polym. Phys. Ed.* **1973**, *11*, 1385–1411.

(10) Sorensen, R. A.; Liau, W. B.; Boyd, R. H. *Macromolecules* **1988**, *21*, 194–199.

(11) Sorensen, R. A.; Liau, W. B.; Kesner, L.; Boyd, R. H. *Macromolecules* **1988**, *21*, 200–208.

(12) Boyd, R. H.; Kesner, L. *Macromolecules* **1987**, *20*, 1802–1806.

(13) Blaisdell, J. J.; Sokalski, W. A.; Hariharan, P. C.; Kaufman, J. J. *J. Non-Cryst. Solids* **1985**, *75*, 319–325.

(14) Elias, H.-G. *Macromolecules, Volume 1: Structure and Properties*, 2nd ed.; Plenum Press: New York, 1984.

(15) Wessling, R. A.; Harrison, I. R., private communication.

(16) Narita, S.; Okuda, K. *J. Polym. Sci.* **1959**, *38*, 270–272.